Am J Physiol Heart Circ Physiol 291: H403–H412, 2006.
First published January 20, 2006; doi:10.1152/ajpheart.01240.2005.

Single-beat estimation of end-diastolic pressure-volume relationship: a novel method with potential for noninvasive application

Stefan Klotz,[1] Ilan Hay,[1] Marc L. Dickstein,[2] Geng-Hua Yi,[1] Jie Wang,[1] Mathew S. Maurer,[1] David A. Kass,[3] and Daniel Burkhoff[1]

[1]*Departments of Medicine and* [2]*Anesthesiology, College of Physicians and Surgeons, Columbia University, New York City, New York; and* [3]*Department of Medicine, John Hopkins Medical Institutions, Baltimore, Maryland*

Submitted 23 November 2005; accepted in final form 12 January 2006

Klotz, Stefan, Ilan Hay, Marc L. Dickstein, Geng-Hua Yi, Jie Wang, Mathew S. Maurer, David A. Kass, and Daniel Burkhoff. Single-beat estimation of end-diastolic pressure-volume relationship: a novel method with potential for noninvasive application. *Am J Physiol Heart Circ Physiol* 291: H403–H412, 2006. First published January 20, 2006; doi:10.1152/ajpheart.01240.2005.—Whereas end-systolic and end-diastolic pressure-volume relations (ESPVR, EDPVR) characterize left ventricular (LV) pump properties, clinical utility of these relations has been hampered by the need for invasive measurements over a range of pressure and volumes. We propose a single-beat approach to estimate the whole EDPVR from one measured volume-pressure (V_m and P_m) point. Ex vivo EDPVRs were measured from 80 human hearts of different etiologies (normal, congestive heart failure, left ventricular assist device support). Independent of etiology, when EDPVRs were normalized ($EDPVR_n$) by appropriate scaling of LV volumes, $EDPVR_n$s were nearly identical and were optimally described by the relation $EDP = A_n \cdot EDV^{B_n}$, with $A_n = 28.2$ mmHg and $B_n = 2.79$. V_0 (the volume at the pressure of ~0 mmHg) was predicted by using the relation $V_0 = V_m \cdot (0.6 - 0.006 \cdot P_m)$ and V_{30} by $V_{30} = V_0 + (V_{m,n} - V_0)/(P_m/A_n)^{(1/B_n)}$. The entire EDPVR of an individual heart was then predicted by forcing the curve through V_m, P_m, and the predicted V_0 and V_{30}. This technique was applied prospectively to the ex vivo human EDPVRs not used in determining optimal A_n and B_n values and to 36 in vivo human, 12 acute and 14 chronic canine, and 80 in vivo and ex vivo rat studies. The root-mean-square error (RMSE) in pressure between measured and predicted EDPVRs over the range of 0–40 mmHg was <3 mmHg of measured EDPVR in all settings, indicating a good predictive value of this approach. Volume-normalized EDPVRs have a common shape, despite different etiology and species. This allows the entire curve to be predicted by a new method with a potential for noninvasive application. The results are most accurate when applied to groups of hearts rather than to individual hearts.

cardiovascular disease; diagnostic techniques

THE LEFT VENTRICULAR (LV) end-diastolic pressure-volume relationship (EDPVR) is the most important means of characterizing passive ventricular properties, in that it is the global, integrated expression of chamber geometry, wall thickness, and all aspects of passive material properties of the myocardial wall. By definition, the EDPVR indicates the amount of diastolic filling that will occur for a specified filling pressure and is therefore a key physiological determinant of preload (10, 13). In addition, assessment of this relationship is fundamental to the study of the pathophysiology of ventricular remodeling in heart failure and in response to surgical, pharmacological, or device-based treatment strategies (8, 11, 14, 21).

Most studies of the EDPVR have been undertaken in ex vivo models of either beating or arrested hearts in which a balloon is placed in the LV chamber and volume is varied while pressure is measured (5, 12, 22). In vivo assessment of the EDPVR requires use of a means of continuous volume measurement, such as a conductance catheter or multidimensional sonomicrometry, during transient inferior vena caval occlusion (IVCO) (1, 2, 15). For human subjects, the conductance catheter technique is the only feasible volume measurement technique for this purpose. However, required use of invasive techniques to assess the EDPVR has limited its clinical utility in patients.

Until recently, measurement of the end-systolic pressure-volume relationship (ESPVR) also required continuous invasive pressure-volume measurements over a range of volumes created by IVCO. However, Sunagawa and colleagues (25) and Kass and colleagues (7, 24) suggested means of estimating the entire ESPVR from measurement of pressure-volume data from a single beat. Kass and colleagues developed and validated a noninvasive approach in patients from measurements of blood pressure (sphymometry), ventricular volumes (e.g., echocardiography, radionucleotide ventriculography), and Doppler-derived measurements of specific time intervals of the cardiac cycle (7, 24). Such approaches have the potential to overcome the obstacles that have impeded more widespread use of the pressure-volume approach in studies of ventricular mechanics in health and disease. Availability of a comparable approach for assessing the EDPVR would be another major step toward achieving this goal.

We obtained ex vivo EDPVRs from normal and diseased human hearts having a very wide range of heart sizes. We derived an algorithm for normalizing ventricular volume that yielded volume-normalized EDPVRs from all hearts that were very similar to each other. This indicated the existence of a common underlying shape of the EDPVR, independent of heart condition, which can be expressed by a simple analytical expression. This same equation was also shown to be relevant for hearts of normal and diseased animals. It is demonstrated how this analytical equation yields a strategy for predicting the whole EDPVR from a single end-diastolic pressure-volume point. Finally, this approach was validated using the data obtained from in vivo normal and failing hearts of humans, dogs, and rats.

Address for reprint requests and other correspondence: D. Burkhoff, The Jack H. Skirball Center for Cardiovascular Research, Cardiovascular Research Foundation, 8 Corporate Dr., Orangeburg, NY 10962 (e-mail: dburkhoff@crf.org).

The costs of publication of this article were defrayed in part by the payment of page charges. The article must therefore be hereby marked "*advertisement*" in accordance with 18 U.S.C. Section 1734 solely to indicate this fact.

METHODS

Human Heart Harvest and Ex Vivo Pressure-Volume Relationships

Eighty freshly harvested human hearts were obtained for the study. Hearts were from five normal subjects not suitable for transplantation, 23 transplant patients with ischemic cardiomyopathy, 30 transplant patients with idiopathic cardiomyopathy, and 22 patients with end-stage cardiomyopathy supported with an LV assist device (LVAD, TCI HeartMate, Thoratec, Pleasanton, CA, average length of support, 114 ± 86 days). All hearts were perfused with cold hypocalcemic, hyperkalemic cardioplegia solution at explant. The passive LV pressure-volume relationship of each arrested heart was measured as described previously with an intraventricular balloon (4).

In Vivo Human Experiments

Single-beat estimation of EDPVR was tested by using in vivo human data from 10 healthy old and 13 healthy young controls and from 13 patients with heart failure and a normal ejection fraction (HFNEF). The in vivo EDPVRs were constructed by conductance catheter technique using transient inferior vena caval occlusion as described in detail previously (7, 20, 24).

In Vivo Canine Experiments

Data were also obtained from 12 open chest dogs and from 14 chronically instrumented awake dogs. In the chronically instrumented dogs, data were available from each dog under normal conditions and following induction of heart failure by repeated coronary embolization (23).

For acute experiments, LV pressure (LVP) was measured by a catheter tip micromanometer (Millar, Houston, TX) placed inside the LV from the right or left carotid artery. A plastic balloon occluder was placed around the inferior vena cava for temporary occlusion (IVCO). Six ultrasound crystals were positioned in the midmyocardium (3 pairs to measure anterior-to-posterior, base-to-apex and septum-to-lateral wall distances) to estimate LV volume (LVV) based on an ellipsoidal model: $LVV = \pi/6(a \cdot b \cdot c)$, where a, b, and c are the principle axis dimensions.

For chronic experiments, animals were instrumented with an indwelling pressure gauge (Konigsberg), sonomicrometer crystals, and an balloon occluder around the inferior vena cava as described previously (28). LVV was obtained the same way as in acute experiments. Measurements of EDPVRs were obtained in a conscious state of the animal by transient IVCO at baseline and 4 wk after induction of heart failure by repeated, daily intracoronary microsphere embolization.

Ex Vivo and In Vivo Rat Experiments

Data were also obtained from Sprague-Dawley rats in heart failure 6 and 12 wk after coronary artery ligation ($n = 58$) and in 22 normal control rats. For in vivo assessment of the LV passive pressure-volume characteristics, the rats were intubated after induction of anesthesia with isoflurane, and the right carotid artery was cannulated with a Millar conductance catheter (Millar Instruments, Houston, TX). LV EDPVRs were performed by temporary IVCO. For ex vivo assessment of the LV passive pressure-volume characteristics, the heart was arrested in diastole and excised quickly. The left atrium was opened, and a thin latex balloon was attached to the end of a 10-cm length of stiff polyethylene tubing with fenestrations at the distal 3 mm of its tip. LVP was measured using a 5-Fr Millar micromanometer as volume was infused into the balloon at 0.025-ml increments.

All procedures involving human hearts were approved by the Institutional Review Board of Columbia University and the John Hopkins Medical Institutions. All animals involved in these studies received humane care in compliance with the *Guide for the Care and Use of Laboratory Animals* published by the National Institutes of Health (NIH Publication No. 85-23, Revised 1996). These studies were approved by the Institutional Animal Care and Use Committee of Columbia University.

Theoretical Considerations

EDPVR analysis. Although human, canine, and rat hearts in different states (normal, failing, and post-LVAD) have very different sizes, earlier studies have shown that EDPVRs from such hearts can all generally be described by one of several nonlinear analytical expressions (e.g., $EDP = \alpha \cdot EDV^{\beta}$ or $EDP = \alpha \cdot e^{\beta \cdot EDV}$) with different coefficient values (17). This suggests that EDPVRs share a common underlying shape and that, if appropriately scaled using a single descriptive equation, the curves may converge. To test this hypothesis, ex vivo EDPVRs from humans were normalized ($EDPVR_n$) in the volume dimension to account for the unstressed volume (V_0, volume at which EDP is ~0 mmHg) and V_{30}, the volume at which EDP equals 30 mmHg, according to the following equation:

$$EDV_n = (EDV - V_0)/(V_{30} - V_0) \quad (1)$$

The resulting $EDPVR_n$s obtained from the experiments outlined above were superimposed to visually determine their degree of similarity. After having established qualitatively that indeed a relatively high degree of similarity exists among these normalized curves, we proposed that the ex vivo $EDPVR_n$s from different groups (human, canine, and rat hearts) could be described by a function with a single universal set of parameter values (A_n, B_n) for the function:

$$EDP = A_n \cdot EDV_n^{B_n} \quad (2)$$

which optimally describe the data (least-square method using commercially available software; IgorPro 4.1, WaveMatrics, Lake Oswego, OR).

Single-beat approach to predicting EDPVR. As will be shown, data indicated the $EDPVR_n$s were similar from ex vivo human, dog, and rat hearts, and curve fitting yielded essentially the same values for A_n and B_n in the different species, indicating a common underlying shape of the EDPVR. From this observation, it is possible to predict the entire EDPVR from a single point on the curve as detailed forthwith.

The procedure starts with measurement of EDP and EDV on a single beat (P_m, V_m, respectively). Based on *Eq. 1*, normalized measured volume ($V_{m,n}$) is defined as follows:

$$V_{m,n} = (V_m - V_0)/(V_{30} - V_0) \quad (3)$$

The resulting $V_{m,n}$-P_m point would fall on the curve:

$$P_m = A_n \cdot V_{m,n}^{B_n} \quad (4)$$

Solving *Eq. 4* for $V_{m,n}$, substituting the result into *Eq. 3*, and solving for V_{30} yields:

$$V_{30} = V_0 + (V_{m,n} - V_0)/(P_m/A_n)^{(1/B_n)} \quad (5)$$

To predict the EDPVR, a reasonable estimate of V_0 is required. The relative constancy of the shape of the normalized EDPVR further suggested a relatively consistent relationship between the volume at a certain pressure and V_0. To test this, we determined the volumes from each human ex vivo heart that provided pressures of 10, 15, 20, and 25 mmHg. These volumes designated V_{10}, V_{15}, V_{20}, and V_{25}, respectively, were each separately plotted versus the V_0 determined from each measured EDPVR (Fig. 1). For each plot, we determined the linear regression equation forced through the origin:

$$V_0 = k \cdot V_m \quad (6)$$

The value of k obtained at each pressure level was then plotted as a function of P_m, and linear regression analysis was applied with the following result:

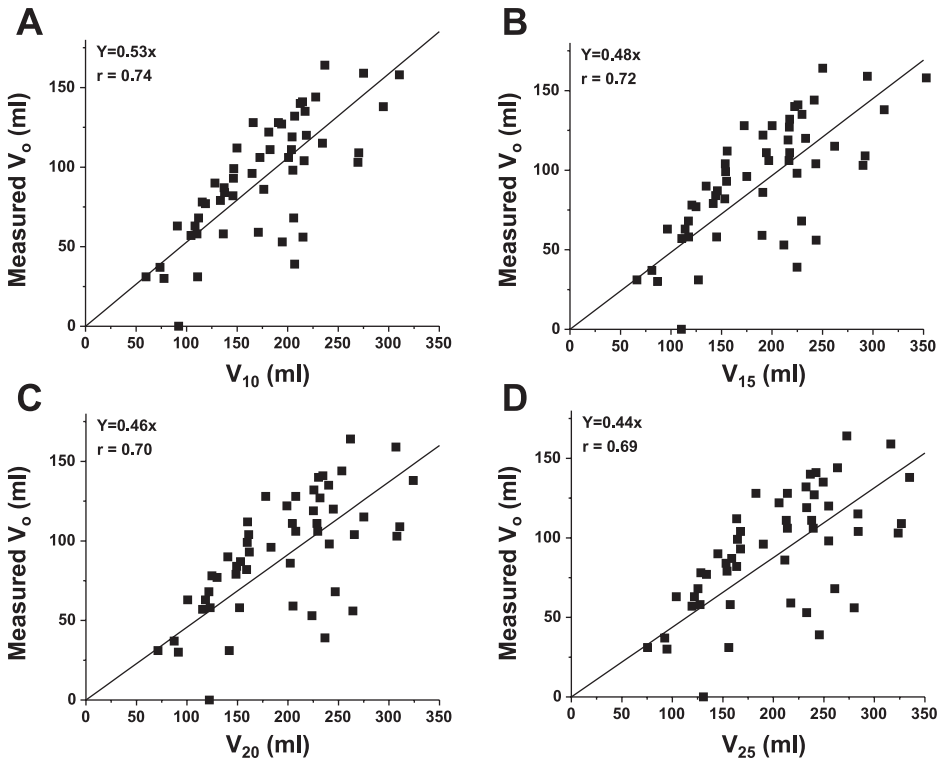

Fig. 1. Volume at 0 mmHg (V_0) measured from human hearts as a function of volume at filling pressures of 10 (V_{10}) (*A*), 15 (V_{15}) (*B*), 20 (V_{20}) (*C*), and 25 mmHg (V_{25}) (*D*). Slopes of regression lines are also shown. Slope (k) was then plotted as a function of the respective filling pressure to yield the result that, on average, $V_0 \approx V_m\,(0.6 - 0.006 \cdot P_m)$, where V_m and P_m are measured volume and pressure points, respectively.

$$k = 0.6 - 0.006 \cdot P_m \quad (7)$$

Substitution of *Eq. 7* into *Eq. 6* yields:

$$V_0 = V_m(0.6 - 0.006 \cdot P_m) \quad (8)$$

The entire EDPVR of an individual heart can then be predicted from analytical determination of α and β to force the curve through the measured point on the EDPVR and the predicted V_0 (*Eq. 8*) and V_{30} (*Eq. 5*) according to the following:

$$\alpha = 30/V_{30}^{\{[\mathrm{Log}(P_m/30)]/[\mathrm{Log}(V_m/V_{30})]\}} \quad (9)$$

$$\beta = [\mathrm{Log}(P_m/30)/\mathrm{Log}(V_m/V_{30})] \quad (10)$$

Thus the final sequence of calculations from a single set of P_m and V_m values would be: *1*) calculate V_0 from *Eq. 8*; *2*) calculate V_{30} from *Eq. 5*; *3*) calculate α and β from *Eqs. 9* and *10*; and *4*) use these estimates of α and β to specify the entire EDPVR by:

$$EDP = \alpha \cdot EDV^{\beta} \quad (11)$$

To test this approach, half of the ex vivo human EDPVRs (*group 1*) chosen at random were used to determine optimal values for A_n and B_n. The predictive power was then tested on the remaining ex vivo human EDPVRs (*group 2*). The approach was then further tested prospectively by using data obtained from in vivo human and canine and ex vivo and in vivo rat studies, again using the A_n and B_n values obtained from *group 1* ex vivo human hearts.

Statistical Methods

Results are expressed as means ± SD. Root-mean-square error (RMSE) between measured and predicted pressures over the entire EDPVR was calculated for each heart as $[\Sigma(P_m - P_p)^2]^{1/2}$ with the summation performed over each measured pressure-volume point. One-way ANOVA was used to detect significant differences in RMSE values among the different groups of hearts (ex vivo and in vivo human hearts, acute dog experiments, chronic dog experiments, and ex vivo and in vivo rat hearts). Dunn's test was used for post hoc multiple comparison. Analyses were performed using commercially available software (SPSS 11.5, Chicago, IL).

RESULTS

Ex Vivo Human Heart Results

Representative examples of EDPVRs measured from ex vivo human hearts are shown in Fig. 2*A*. As shown in these examples, EDPVRs from different types of hearts (normal, idiopathic dilated cardiomyopathy, ischemic cardiomyopathy, post-LVAD) spanned very wide ranges of volumes. Some hearts reached filling pressures of 30 mmHg at as little as ~80 ml, and others reached this same pressure at more than 300 ml. These same EDPVRs are shown in Fig. 2*B* after volume was normalized according to *Eq. 3*. These curves reveal a high degree of concordance between hearts in these different states.

Figure 3 shows data from all 80 human $EDPVR_n$s superimposed on each other. As shown, there is relatively little deviation of these normalized data around a common curve. Optimal A_n and B_n values (±SD) obtained from the group as a whole were 27.8 ± 0.3 and 2.76 ± 0.05, respectively. Furthermore, although the amount of data available from normal hearts is fairly limited, A_n and B_n were similar between normal and cardiomyopathic hearts ($P > 0.7$).

Optimal A_n and B_n from a randomly selected subset of 40 of the ex vivo human hearts (designated as *group 1*) were 28.2 and 2.79 mmHg, respectively, which where very similar to those obtained from the group as a whole. These parameter values were used prospectively to predict the EDPVRs in the remaining ex vivo human data (designated as *group 2*). Representative examples of EDPVR predictions of ex vivo data are shown in Fig. 4, *A–D*. In each panel, the open circles show the measured end-diastolic pressure-volume points. The open

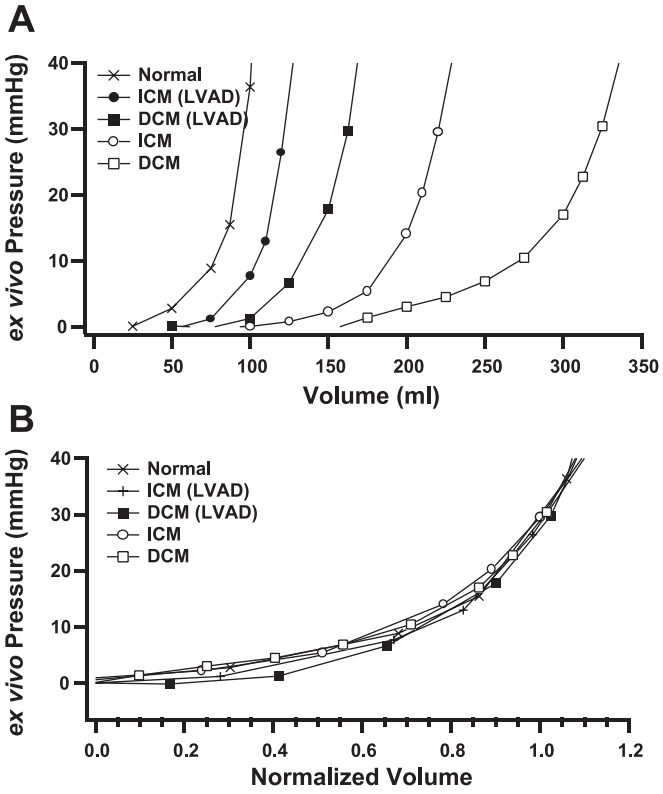

Fig. 2. *A*: examples of end-diastolic pressure-volume relations (EDPVRs) measured from ex vivo human hearts. These EDPVRs spanned very wide ranges of volumes from as little as ~80 ml to >300 ml at filling pressures of 30 mmHg. *B*: EDPVRs from *A* normalized to volume and superimposed on each other. Despite different diseases, the volume-normalized shape of the curves is the same. ICM, ischemic cardiomyopathy; DCM, idiopathic dilated cardiomyopathy; LVAD, hearts supported with a left ventricular assist device.

square shows an end-diastolic pressure-volume point at an EDP of ~15 mmHg selected for the test (i.e., these are P_m and V_m for *Eqs. 9* and *10*). The dotted line shows the curve fit from the raw data using a nonlinear analytic expression ($EDP = P_0 + \alpha \cdot EDV^{\beta}$). The solid line shows the EDPVR predicted from *Eqs. 9, 10,* and *11*. The average RMSE between measured and predicted EDPVRs from the 40 hearts used for the test was 1.74 ± 1.2 mmHg. Figure 4, *A* and *B*, shows examples for which the RMSE between measured and predicted EDPVRs was close to the average for the overall group; these results, which are indicative of the average results, reveal a good predictive capability of the approach. Note in these two examples that the predicted V_{30} point is very close to the measured value. Figure 4*C* shows an example with a very low RMSE value (0.51 mmHg, among the best predictions), whereas Fig. 4*D* shows an example with one of the highest RMSE values (5.70 mmHg, among the worst predictions). Interestingly, we did not find any differences in the predictive capability of this approach among the different types of hearts studied (i.e., chronic heart failure, post-LVAD, or normal control hearts).

The overall accuracy of this approach to predict V_0 (*Eq. 8*) and V_{30} (*Eq. 5*) is summarized in Fig. 5 and Table 1 for *group 2* ex vivo human hearts (Fig. 5*A*) and for hearts of other settings (Fig. 5*B*). As shown, the measured versus predicted V_0 and V_{30}, points fall nearly on the line of identity over the large range of volumes tested (V_0, $R^2 = 0.84$; $P < 0.001$; V_{30}, $R^2 = 0.99$; $P < 0.001$). Overall, predicted V_0 average 5.7 ± 13.7 ml (2.7 ± 20.6%) smaller than measured V_0. Overall, predicted V_{30} averaged 5.6 ± 12.7 ml smaller than measured V_{30}. Examination of this difference in the four groups of Fig. 5*B* (and expressing the difference as a percent to account for the different value ranges) revealed measured V_{30} exceeded predicted V_{30} by 13.5 ± 11.2% in in vivo human hearts, 7.6 ± 6.2% in in vivo chronic dog hearts, and 0.7 ± 3.6% in ex vivo human hearts, whereas for in vivo acute dog hearts average predicted V_{30} was greater the measured V_{30} by 10.4 ± 12.7%. However, multiple linear regression (with group coded as a dummy variable) analysis indicated that the relationship between measured and predicted V_{30} values did not differ significantly between these groups.

We next explored whether the accuracy of the EDPVR prediction depended on the range within which the measured end-diastolic pressure point falls. RMSE between measured and predicted EDPVRs were obtained from all ex vivo EDPVRs at different pressure points (~10, ~15, and ~20 mmHg). Figure 6 shows that when a measured pressure-volume point having an EDP above 15 mmHg is used to predict the EDPVR, the prediction is better than when it is predicted by a point having an EDP of 10 mmHg or less ($P < 0.05$ 10 mmHg vs. 15 and 20 mmHg).

In Vivo Human Hearts

EDPVRs were measured from 36 human hearts in vivo by using the conductance catheter technique of volume measurement and transient IVCO to reduce preload. The EDP-EDV from the starting loop (i.e., before IVCO) were the designated P_m and V_m values for EDPVR prediction. Overall, the average RMSE obtained from the 36 EDPVRs was 2.99 ± 1.72 mmHg. Four examples (two average, one above average, and one of the worst examples) are shown in Fig. 7, *A–D*, respectively. The example showing the worst predictive value (Fig. 7*D*) was from a patient with heart failure with normal ejection fraction (HFNEF) in which the EDPVR did not have an asymptote with the *x*-axis, which was considered to be because of high right-sided filling pressures and pericardial mediate interventricular interactions. Another means of assessing the accuracy of the prediction was to compare measured and predicted pressures at an intermediate volume, e.g., at a volume yielding 15 or 20 mmHg, V_{15} and V_{20}, respectively. For these in vivo human hearts, measured versus predicted V_{15} was 113 ± 27 vs. 110 ±

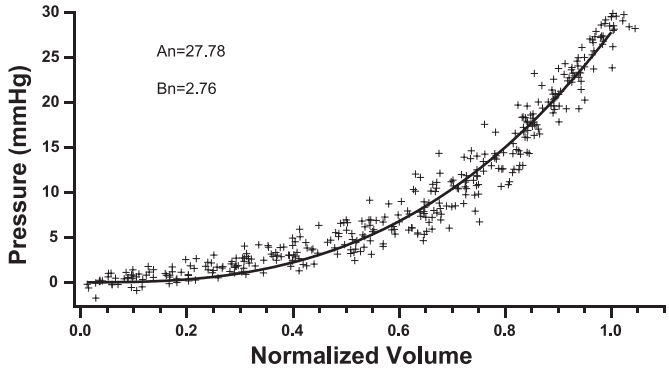

Fig. 3. All ex vivo human volume-normalized EDPVR data shown superimposed on each other. A_n and B_n, parameter values.

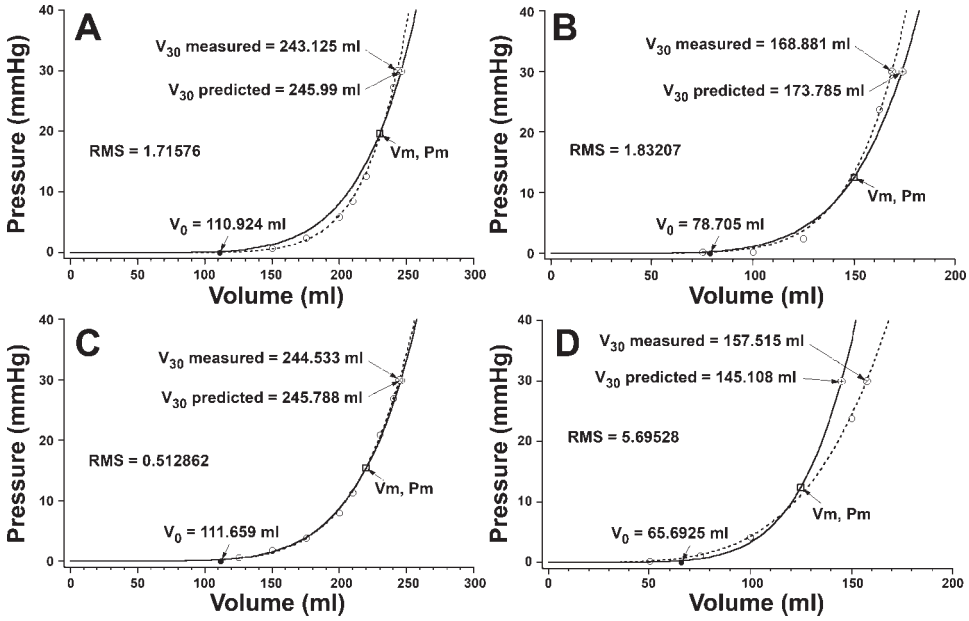

Fig. 4. Different examples of the single-beat estimation to predict V_{30} and the entire EDPVR from ex vivo human data. Open circles, end-diastolic pressure-volume points measured ex vivo from the heart. Open squares, end-diastolic pressure-volume point at an end-diastolic pressure of ~15 mmHg selected for prediction (V_m and P_m from *Eqs. 9* and *10* in text). Dotted line, curve fit from the raw data using a nonlinear analytic expression. Solid line, entire EDPVR with parameter values predicted from *Eq. 2*. circled plus sign (⊕), V_{30} on the best-fit EDPVR; circled cross (⊗), predicted V_{30}. *A* and *B*: EDPVR prediction with a root-mean-square error (RMSE) value around the average; *C*: EDPVR prediction with an RMSE value above average; *D*: EDPVR prediction with a very high RMSE.

27 ml, and for V_{20} these numbers were 120 ± 28 vs. 115 ± 29, differences of only 3–5 ml or less than a 5% error.

Other Species

To explore the overall general applicability of this approach, data from acute and chronic in vivo dog hearts and in vivo and ex vivo rat hearts were also explored. Plots comparable to those of Fig. 3 revealed similar behavior in each of these settings and, remarkably, the parameter values for A_n and B_n were nearly identical to those identified in the ex vivo human hearts (Table 1). Also shown in Table 1, the means ± SD RMSE values between measured and predicted EDPVRs and the regression coefficients for the relationship between measured and predicted V_{30} values for all groups were also, in general, comparable among these different settings so that prospective EDPVR predictions (Fig. 8) were generally excellent. The RMSE values for in vivo human and chronic dog hearts were slightly higher than those attained in the other settings, but the values were still relatively small, indicating good prospective predictive capability of this approach.

Sensitivity Analysis

It is pertinent to ask about the sensitivity of the predicted curves to potential inaccuracies in measurement of pressures and volumes, particularly for the clinical scenario when both parameters may be measured noninvasively. Of course, any technique for measuring the EDPVR is equally sensitive to the methods used to measure both pressure and volume. Such an analysis is relatively straightforward because of the simple analytical nature of the prediction algorithm, therefore, for the sake of brevity, only two important examples involving errors in P_m variation are considered in this section; a similar analysis of error in V_m yields similar findings. Figure 9 shows EDPVRs predicted from a common V_m of 100 ml and P_m values of 16 mmHg along with P_m values of 14 and 18 mmHg and 13 and 19 mmHg (i.e., 16 ± 2 and 16 ± 3 mmHg). As seen, the impact is relatively minor if one were interested in determining

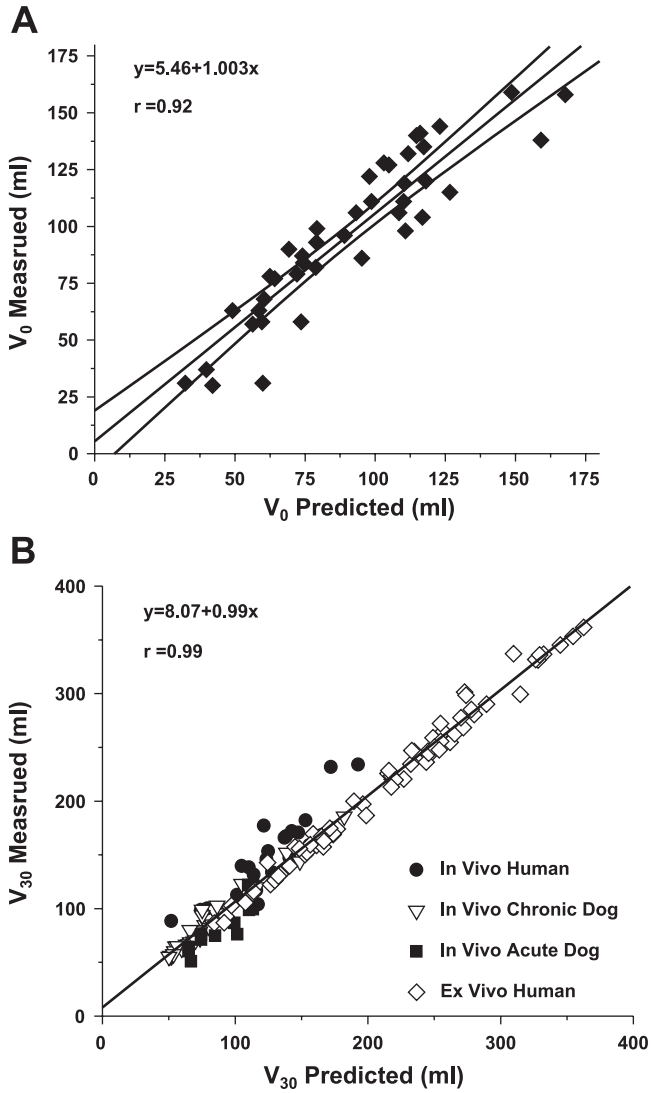

Fig. 5. Correlation plots of the agreement between measured and predicted V_0 (*A*) and V_{30} (*B*).

Table 1. *A_n and B_n values derived from each experimental setting along with RMSE values and correlation coefficient between measured and predicted V_{30}*

	A_n, mmHg	B_n	RMSE, mmHg	R^2 (V_{30})
Ex vivo				
Human	27.8	2.76	1.74±1.19*	0.99546
Rat	28.3	2.67	1.76±0.79*	0.99786
In vivo				
Human			2.99±1.72	0.89058
Chronic dog			3.02±1.44	0.97833
Acute dog			1.07±0.65*	0.88961
Rat			1.02±0.66*	0.96741

All values are means ± SD. RMSE, root-mean-square error in estimate of pressures. R^2, correlation coefficient; A_n and B_n, parameter values. *$P < 0.05$ vs. in vivo human and chronic dog.

ventricular capacitance. For example, consider an arbitrary clinical application in which one desired to define capacitance as the volume at a pressure of either 10, 15, or 20 mmHg (V_{10}, V_{15}, V_{20}, respectively). In this example, the 6-mmHg range of possible errors of specifying P_m would result in only an ~6 ml range of predicted V_{10}, V_{15}, or V_{20}, which amounts to a range of approximately ±3%.

Next consider the potentially more difficult example in which data from groups of normal and heart failure patients may be compared. In such a case, P_m may be in the range of 12 mmHg and V_m in the range of 100 ml in the normal group and 24 mmHg and 225 ml, respectively, in a group of patients with heart failure due to systolic dysfunction. Figure 9*B* shows predicted EDPVRs at these values of V_m and P_m along with those obtained with P_m values ±3 mmHg. The graphs show that even with errors of this magnitude and despite performing estimates from different pressure ranges, information regarding the EDPVR is relatively consistent. More specifically, in the heart failure state, the value of capacitance (volume at a given pressure) is influenced similarly in the simulated failing and normal states (except in the low pressure range). However, the shape of the EDPVR (which would relate more directly to an estimate of chamber compliance and stiffness) is more significantly influenced in the heart failure state, especially in the low pressure range.

Another important aspect of the prediction algorithm is the estimation of V_0 using *Eq. 8*, which can be associated with significant uncertainty and inaccuracy especially as the volume of the heart increase as in systolic heart failure. Figure 9*C* shows a hypothetical example with an assumed V_m of 200 ml at a P_m of 10 mmHg. *Equation 9* predicts a V_0 of 108, but based on Fig. 1, V_0 could exhibit considerable variability. The three graphs of Fig. 9*C* show EDPVR predictions with V_0 values of 75, 100, and 125 ml. Despite this rather large variation in the assumed V_0 value, the impact on predicted EDPVR is relatively mild.

DISCUSSION

We developed and tested a novel method for estimating the EDPVR from a single end-diastolic pressure-volume point. From the availability of Doppler-echocardiography (6, 18), radionuclide ventriculography (3, 27), and magnetic resonance (9) imaging methods to estimate ventricular pressures and volumes, this approach to EDPVR estimation has the possibility of being utilized noninvasively. Interestingly, though developed primarily based on data from human hearts, the approach appears to be generally applicable to normal and diseased hearts of different species. Values of RMSE ranging between 0.5 and 6 mmHg among all these hearts (Table 1) indicate that, on average, the predicted EDPVR falls within 1.8 mmHg of the actual EDPVR over a range of conditions.

The proposed single-beat EDPVR estimation method is based on the premise that the end-diastolic pressure-volume relation can generally be described by common nonlinear analytical expressions with coefficient values that are reasonably well linked with the size of the heart (17). This suggests that overall these EDPVRs share a common underlying shape. The present results are intended to facilitate the use of the EDPVR in clinical and research settings where assessment of changes in passive ventricular properties are important, such as in certain disease states and following therapeutic interventions. The prospective prediction of EDPVRs measured in vivo using the conductance catheter technique combined with transient inferior vena caval occlusion serve as important validation of the approach.

The low RMSE values between measured and predicted EDPVRs indicate good predictive accuracy of the approach. The accuracy was greatest when the pressure of the single measured end-diastolic pressure-volume point existed within a pressure range over 15 mmHg. Specifically with regard to the clinical situation, this single-beat approach provided a predicted EDPVR that was on average within ~3 mmHg of that measured in humans using the conductance technique.

Taken to the extreme, the underlying assumption that the EDPVR of all hearts share a common underlying shape regardless of species or disease state would lead to the conclusions that passive myocardial properties and chamber geometry change in only one way and that any two hearts that have a single common end-diastolic pressure-volume point would have identical EDPVRs. However, consider even the extreme case shown in Fig. 4*D*. In this example, measured and predicted values of α and β are considerably different. Despite such deviations, which reflect expected variations in material properties and geometry, the differences between the actual

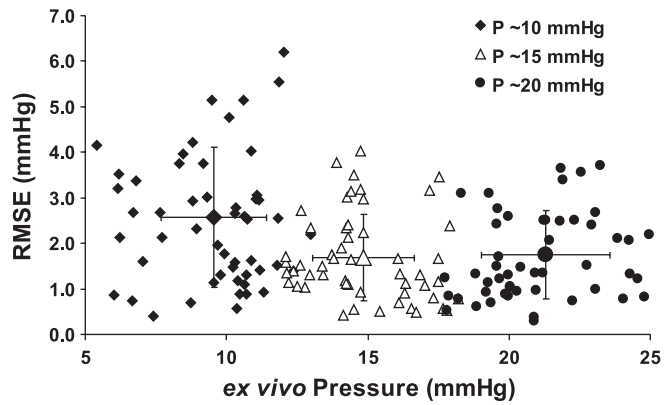

Fig. 6. Correlation between chosen pressure point and RMSE values in prediction of ex vivo human EDPVRs. EDPVR prediction by choosing a pressure-volume point (P) around 10 mmHg is not as accurate as between 15 and 20 mmHg. Large square, triangle, and circle are means ± SD. *$P < 0.05$ vs. 15 and 20 mmHg

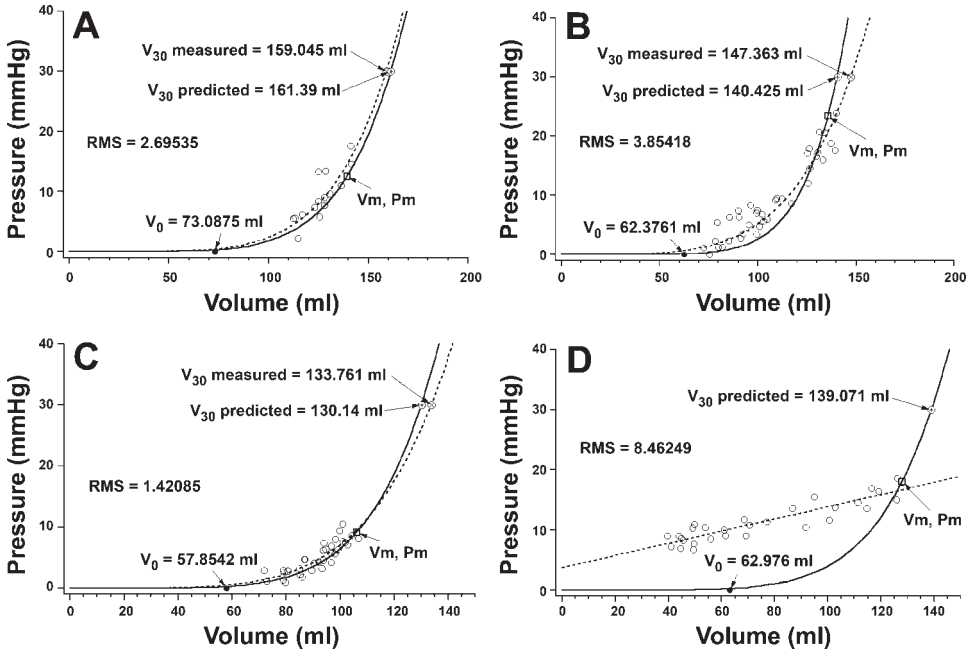

Fig. 7. Four examples of single-beat estimation of entire EDPVR from in vivo human data. *A* and *B*: EDPVR prediction with a RMSE value around average. *C*: EDPVR prediction with a RMSE value above average; *D*: EDPVR prediction with a very high RMSE. Format as detailed for legend for Fig. 4. See text for further details.

and predicted EDPVRs are relatively small. The average results indicate that the expected deviation between predicted and measured EDPVR curves is typically <3 mmHg. Nevertheless, this means that results obtained using the proposed approach would be most accurate when applied to groups of hearts (where such deviations would average out), rather than to individual hearts.

To illustrate this point, consider the example shown in Fig. 10. Little et al. (16) provided group-average end-diastolic pressure-volume data in Table 1 of their publication. These data were obtained in an experimental canine preparation in which volumes were measured by sonomicrometry and pressure measured by a solid-state transducer over a range of conditions achieved by phenylephrine administration. These data, which are rarely provided in published papers, were plotted and the EDPVR predicted using the proposed approach. This completely independent data suggest that the proposed approach is reasonable. We propose that one potentially important use of this approach is in a research setting in which group-averaged EDPVRs from different groups are to be estimated and compared.

Several prior studies have reported methods for single-beat estimation of the end-systolic pressure-volume relationship (ESPVR) with good predictions of end-systolic elastance (7, 24, 26). The linearity of the ESPVR simplifies in some ways its prediction. The inherent nonlinearity of the EDPVR makes its prediction with a single beat approach more difficult. However, the common shape of this curve and uniformity following

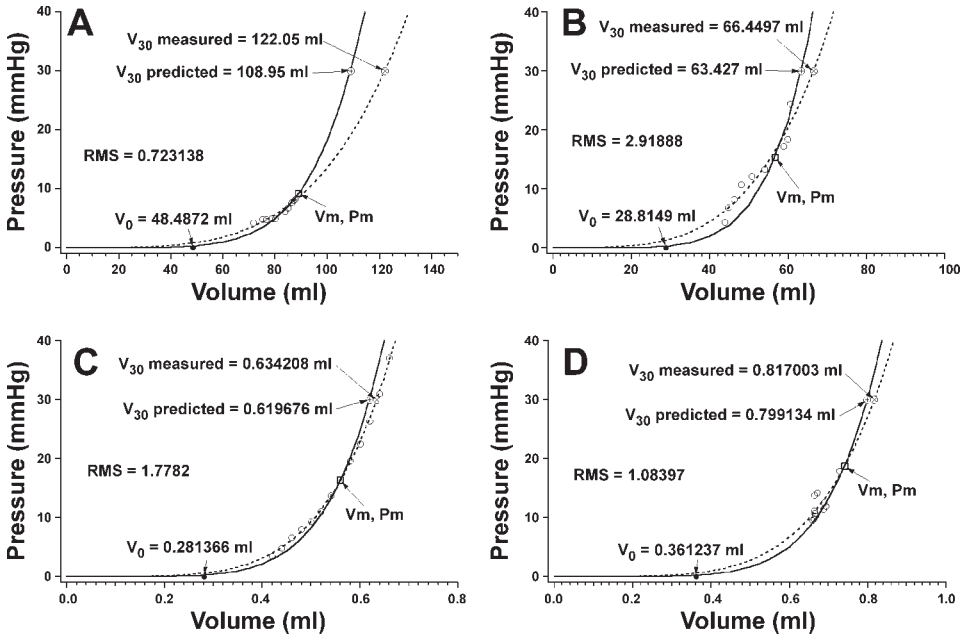

Fig. 8. Representative examples of single-beat estimation of entire EDPVR from in vivo acute dog (*A*), in vivo chronic dog (*B*), ex vivo rat (*C*), and in vivo rats (*D*) data. Overall, a high prediction capability was observed with the same equation and parameter values despite different species and heart sizes. Format as detailed for legend for Fig. 4. See text for further details.

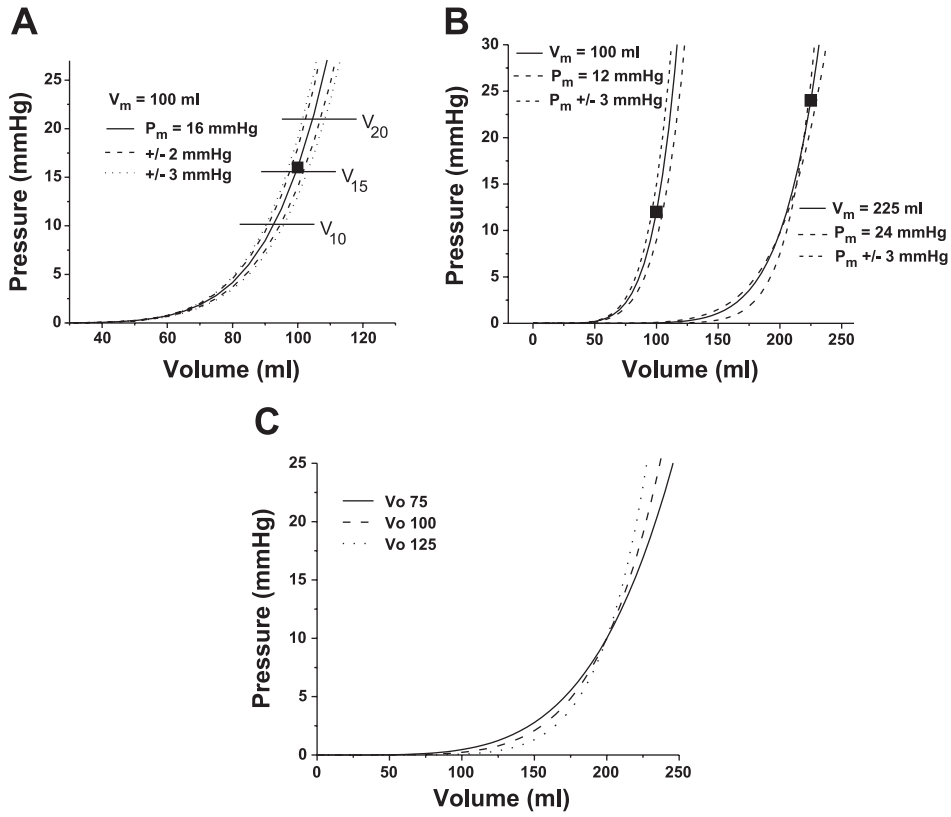

Fig. 9. Examples of sensitivity to of EDPVR predictions to errors in measurement of end-diastolic pressure. *A*: EDPVRs predicted at V_m of 100 ml and P_m of 16 mmHg showing impact of ± 2 and ± 3 mmHg errors. Dashed lines, pressure levels at which volumes at pressures of 10, 15, and 20 mmHg would be identified. *B*: hypothetical EDPVRs predicted in normal hearts (with V_m 100 ml and P_m 12 mmHg) and from a patient with systolic heart failure (with V_m 225 ml and P_m 24 mmHg) along with impact of ±3 mmHg errors in pressure estimates. *C*: impact of errors in V_0 estimation on EDPVR prediction. See text for details.

volume normalization procedure allowed description of a simple method of EDPVR prediction.

In practice, the proposed scheme for predicting the EDPVR can be accomplished noninvasively. Methods for measurement of LV volume include magnetic resonance imaging, three-dimensional echocardiography, and radionuclide ventriculography (3, 29, 30). Measurement of pulmonary vein velocity by Doppler-echocardiographic techniques provides a means of estimating LV EDP (19).

Study Limitations

The correlation between predicted and measured points was excellent in all ex vivo setups and in vivo acute dogs and rats, measured with sonomicrometry and conductance techniques, respectively. These experimental settings offer ideal conditions in which confounding factors (e.g., controlling respiration) are minimized, and the ability to vary volumes and pressures over a broad range is possible. The good, but slightly lower, correlation obtained from in vivo chronic conscious dog and human data may reflect the effects of respiration and possibly effects of interventricular interactions and pericardial constraints, which may result in an EDPVR that does not have an asymptote with the volume axis (as in Fig. 7*D*). However, these factors did not impair the ability of the overall approach to provide good predictions in a majority of cases. Such factors could become more important in disease states where right ventricular overload is more prominent and thus limit the utility of the present approach.

The values of A_n and B_n were obtained from normal and dilated cardiomyopathic hearts, which may limit the applicability of the approach to other disease states. Nevertheless, the approach appeared to apply well in vivo to patients even with heart failure and normal ejection fraction due to hypertensive and/or idiopathic hypertrophic cardiomyopathies. This again speaks to the general applicability of the underlying observation that the EDPVR generally has a common shape.

The mathematical form of the equation used to describe the EDPVR ($P = \alpha V^{\beta}$) was chosen because it was the only one of the commonly used equations that lends itself to the analytical solution permitting the current prediction. However, it is cur-

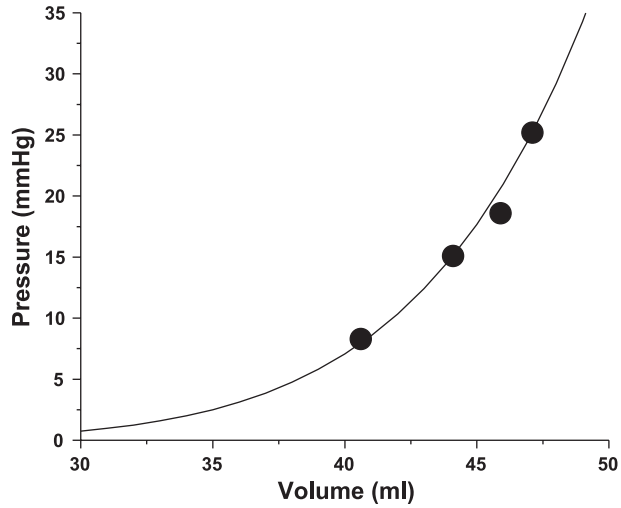

Fig. 10. Group-averaged canine end-diastolic pressure-volume data from Little et al. (circles) (16) were replotted and EDPVR predicted using the proposed method. Prediction (line) matches this group-averaged data (from a completely independent source) quite satisfactorily.

rently more common that an exponential equation be used to describe the EDPVR (e.g., $P = \alpha e^{\beta V}$). Thus the values of α and β generated using the present approach will differ from those now commonly appearing in the literature. For example, typical values for α and β obtained with the present approach would be 1.6×10^{-11} mmHg and 6.0, respectively, for normal human hearts and 4.1×10^{-9} mmHg and 5.8, respectively, for normal dog hearts.

From an analytical perspective, the prediction also depends on a degree of difference between the P_m and 30 mmHg. Thus, for P_m between ~27 and 32 mmHg, the currect predictions break down. Future efforts could also resolve this limitation.

Finally, further consideration should be given to the effects of right-sided filling pressures, pericardial pressures, and ventricular interdependence. This is especially important in the data generated by caval occlusion in which these pressures are changing and can influence the resulting EDPVR. Whereas such effects can be eliminated in studies performed ex vivo (i.e., by completely unloading the RV), these effects are difficult (sometimes impossible) to discern in vivo without the use of special instrumentation (e.g., pericardial pressure measurements). Thus, even when measured invasively with a conductance catheter or by sonomicrometry, interpretation of an EDPVR measured in vivo during caval occlusion is subject to these same limitations.

In addition to potentially addressing these limitations, future efforts could possibly improve the proposed approach. The cornerstone of such efforts should be aimed at obtaining a larger amount of invasive data from human and animal hearts over a range of normal and pathophysiological states. Such data could be used to refine the parameters employed in the prediction method. Among the parameters that could possibly be refined would be those used in the prediction of V_0 in different settings and an attempt to understand the degree to which actually allowing disease-specific differences in the shape of the EDPVR could improve predictive accuracy.

In conclusion, the LV end-diastolic pressure-volume relationship can be reasonably estimated from a single pressure-volume point, and the predicted relationships are generally well correlated with directly measured data. The results obtained are most accurate when applied to groups of hearts rather than to individual hearts. The potential for noninvasive application is particularly appealing and is complementary to the recently proposed approach to single beat estimation of the ESPVR.

REFERENCES

1. **Applegate RJ, Cheng CP, and Little WC.** Simultaneous conductance catheter and dimension assessment of left ventricle volume in the intact animal. *Circulation* 81: 638–648, 1990.
2. **Baan J, van der Velde ET, de Bruin HG, Smeenk GJ, Koops J, van Dijk AD, Temmerman D, Senden J, and Buis B.** Continuous measurement of left ventricular volume in animals and humans by conductance catheter. *Circulation* 70: 812–826, 1984.
3. **Bohn J, Rienmuller R, Seiderer M, and Strauer BE.** Non-invasive determination of the end-diastolic volume of the left ventricle. A comparative angiocardiographic, two-dimensional echocardiographic, computer tomographic and radionuclide ventriculographic study. *Z Kardiol* 72: 438–447, 1983.
4. **Burkhoff D, Flaherty JT, Yue DT, Herskowitz A, Oikawa RY, Sugiura S, Franz MR, Baumgartner WA, Schaefer J, Reitz BA, and Sagawa K.** In vitro studies of isolated supported human hearts. *Heart Vessels* 4: 185–196, 1988.
5. **Burkhoff D, Yue DT, Franz MR, Hunter WC, and Sagawa K.** Mechanical restitution of isolated perfused canine left ventricles. *Am J Physiol Heart Circ Physiol* 246: H8–H16, 1984.
6. **Cecconi M, Manfrin M, Zanoli R, Colonna P, Ruga O, Pangrazi A, and Soro A.** Doppler echocardiographic evaluation of left ventricular end-diastolic pressure in patients with coronary artery disease. *J Am Soc Echocardiogr* 9: 241–250, 1996.
7. **Chen CH, Fetics B, Nevo E, Rochitte CE, Chiou KR, Ding PA, Kawaguchi M, and Kass DA.** Noninvasive single-beat determination of left ventricular end-systolic elastance in humans. *J Am Coll Cardiol* 38: 2028–2034, 2001.
8. **Heerdt PM, Holmes JW, Cai B, Barbone A, Madigan JD, Reiken S, Lee DL, Oz MC, Marks AR, and Burkhoff D.** Chronic unloading by left ventricular assist device reverses contractile dysfunction and alters gene expression in end-stage heart failure. *Circulation* 102: 2713–2719, 2000.
9. **Ichikawa Y, Sakuma H, Kitagawa K, Ishida N, Takeda K, Uemura S, Motoyasu M, Nakano T, and Nozaki A.** Evaluation of left ventricular volumes and ejection fraction using fast steady-state cine MR imaging: comparison with left ventricular angiography. *J Cardiovasc Magn Reson* 5: 333–342, 2003.
10. **Jacob R and Kissling G.** Ventricular pressure-volume relations as the primary basis for evaluation of cardiac mechanics. Return to Frank's diagram. *Basic Res Cardiol* 84: 227–246, 1989.
11. **Kass DA, Baughman KL, Pak PH, Cho PW, Levin HR, Gardner TJ, Halperin HR, Tsitlik JE, and Acker MA.** Reverse remodeling from cardiomyoplasty in human heart failure. External constraint versus active assist. *Circulation* 91: 2314–2318, 1995.
12. **Kil PJ and Schiereck P.** Influence of the velocity of changes in end-diastolic volume on the starling mechanism of isolated left ventricles. *Pflügers Arch* 396: 243–253, 1983.
13. **Laird JD.** Asymptotic slope of log pressure vs log volume as an approximate index of the diastolic elastic properties of the myocardium in man. *Circulation* 53: 443–449, 1976.
14. **Levin HR, Oz MC, Chen JM, Packer M, Rose EA, and Burkhoff D.** Reversal of chronic ventricular dilation in patients with end-stage cardiomyopathy by prolonged mechanical unloading. *Circulation* 91: 2717–2720, 1995.
15. **Little WC, Cheng CP, Mumma M, Igarashi Y, Vinten-Johansen J, and Johnston WE.** Comparison of measures of left ventricular contractile performance derived from pressure-volume loops in conscious dogs. *Circulation* 80: 1378–1387, 1989.
16. **Little WC, Ohno M, Kitzman DW, Thomas JD, and Cheng CP.** Determination of left ventricular chamber stiffness from the time for deceleration of early left ventricular filling. *Circulation* 92: 1933–1939, 1995.
17. **Mirsky I.** Assessment of passive elastic stiffness of cardiac muscle: mathematical concepts, physiologic and clinical considerations, directions of future research. *Prog Cardiovasc Dis* 18: 277–308, 1976.
18. **Neumann A, Soble JS, Anagnos PC, Kagzi M, and Parrillo JE.** Accurate noninvasive estimation of left ventricular end-diastolic pressure: comparison with catheterization. *J Am Soc Echocardiogr* 11: 126–131, 1998.
19. **Olariu A, Wellnhofer E, Grafe M, and Fleck E.** Non-invasive estimation of left ventricular end-diastolic pressure by pulmonary venous flow deceleration time. *Eur J Echocardiogr* 4: 162–168, 2003.
20. **Pak PH, Maughan L, Baughman KL, and Kass DA.** Marked discordance between dynamic and passive diastolic pressure-volume relations in idiopathic hypertrophic cardiomyopathy. *Circulation* 94: 52–60, 1996.
21. **Pouleur H, Rousseau MF, van Eyll C, Stoleru L, Hayashida W, Udelson JA, Dolan N, Kinan D, Gallagher P and Ahn S.** Effects of long-term enalapril therapy on left ventricular diastolic properties in patients with depressed ejection fraction SOLVD Investigators. *Circulation* 88: 481–491, 1993.
22. **Regen DM, Denton PK, Howe WC, Taylor LK, and Hansen DE.** Characteristics of left-ventricular isovolumic pressure waves in isolated dog hearts. *Heart Vessels* 9: 155–166, 1994.
23. **Sabbah HN, Stein PD, Kono T, Gheorghiade M, Levine TB, Jafri S, Hawkins ET, and Goldstein S.** A canine model of chronic heart failure produced by multiple sequential coronary microembolizations. *Am J Physiol Heart Circ Physiol* 260: H1379–H1384, 1991.
24. **Senzaki H, Chen CH, and Kass DA.** Single-beat estimation of end-systolic pressure-volume relation in humans. A new method with the potential for noninvasive application. *Circulation* 94: 2497–2506, 1996.

25. **Shishido T, Hayashi K, Shigemi K, Sato T, Sugimachi M, and Sunagawa K.** Single-beat estimation of end-systolic elastance using bilinearly approximated time-varying elastance curve. *Circulation* 102: 1983–1989, 2000.
26. **Summers RL.** Noninvasive estimation of the end systolic pressure-volume relationship using impedance cardiography. *J Miss State Med Assoc* 41: 575–578, 2000.
27. **Thomsen JH, Patel AK, Rowe BR, Hellman RS, Kosolcharoen P, Feiring AJ, Filipek T, Halama JR, and Polcyn RE.** Estimation of absolute left ventricular volume from gated radionuclide ventriculograms. A method using phase image assisted automated edge detection and two-dimensional echocardiography. *Chest* 84: 6–13, 1983.
28. **Todaka K, Wang J, Yi GH, Knecht M, Stennett R, Packer M, and Burkhoff D.** Impact of exercise training on ventricular properties in a canine model of congestive heart failure. *Am J Physiol Heart Circ Physiol* 272: H1382–H1390, 1997.
29. **Underwood SR, Gill CR, Firmin DN, Klipstein RH, Mohiaddin RH, Rees RS, and Longmore DB.** Left ventricular volume measured rapidly by oblique magnetic resonance imaging. *Br Heart J* 60: 188–195, 1988.
30. **Veljovic M, Sobic-Saranovic DP, Pavlovic S, Kozarevic ND, and Bosnjakovic VB.** A new radionuclide approach for the quantification of left ventricular volumes: the "geometric count based" method. *Nucl Med Commun* 24: 915–924, 2003.